



# Multicolor persistent luminescence realized by persistent color conversion

Yan Xia<sup>a</sup>, Xuanqi Huang<sup>a</sup>, Wufeng Wu<sup>a</sup>, Wanbin Li<sup>a</sup>, Zhanjun Li<sup>a,\*</sup>, Gang Han<sup>b</sup>

<sup>a</sup> Guangdong Key Laboratory of Environmental Pollution and Health, School of Environment, Jinan University, Guangzhou 510632, China

<sup>b</sup> Department of Biochemistry and Molecular Pharmacology, University of Massachusetts Medical School, Worcester, MA 01605, USA

## ARTICLE INFO

### Keywords:

Persistent luminescence  
Afterglow  
Spectral tuning  
Persistent phosphor  
Composite

## ABSTRACT

Spectral tuning is important for the development of persistent phosphors. Here we introduce a color conversion concept to obtain abundant persistent luminescence spectra in addition to existing methods of exploring new matrix and/or dopants. In this study,  $\text{CaAl}_2\text{O}_4:\text{Eu},\text{Nd}$  was chosen as a blue persistent donor phosphor, while  $\text{Lu}_3\text{Al}_5\text{O}_{12}:\text{Ce}$  and other four commercial phosphors were explored as conversion phosphors to obtain colorful persistent luminescence spectra. Both the persistent donor phosphor and conversion phosphors were embedded into resin, forming ternary composite chips to ensure efficient energy transfer. Continuous color tuning were realized by simply changing the mass ratio of the persistent donor phosphor vs. conversion phosphor. Our work will be significant in indicating other persistent/conversion composite materials or nanostructures with abundant spectral properties.

## 1. Introduction

The emission of persistent phosphors can persist for a long time after the cessation of excitation. Persistent luminescence and persistent phosphors are arousing increasing interests and have found abundant applications in night vision materials, security signals, art painting, mechanical stress detection, high energy particle detection, optical information storage, catalysis, analysis, time-resolved bioimaging, etc [1–3]. Apparently, these applications rely on the synthesis of persistent phosphors with abundant spectral properties. Many new phosphors have been reported, usually by developing new matrix and/or new dopants. For example,  $\text{Ca}_{0.2}\text{Mg}_{0.9}\text{Zn}_{0.9}\text{Si}_2\text{O}_6:\text{Eu},\text{Dy},\text{Mn}$  is the first developed persistent phosphor in persistent luminescence imaging [4,5]. Cr-doped gallium oxide related phosphors represents the current dominating ones [6–12]. Novel Cr/Ga-free persistent phosphors are being explored such as  $\text{Zn}_3\text{Ga}_2\text{Ge}_2\text{O}_{10}:\text{Ni}^{2+}$  [13],  $\text{LaAlO}_3:\text{Mn}^{4+},\text{Ge}^{4+}$  [14],  $\text{BaZrSi}_3\text{O}_9:\text{Eu}^{2+},\text{Pr}^{3+}$  [15],  $\text{KGaGeO}_4:\text{Bi}^{3+}$  [16], semiconducting polymer [17], metal organic framework [18], etc. Although a number of new persistent phosphors have been explored, to date,  $\text{CaAl}_2\text{O}_4:\text{Eu},\text{Nd}$  (blue, CAO) and  $\text{SrAl}_2\text{O}_4:\text{Eu},\text{Dy}$  (green) still represents the most efficient commercial ones [19,20].

Regarding spectral tuning, in addition to explore new matrix or dopants, a color conversion strategy has been widely applied in the field of LED lighting to obtain white light [21]. Generally, a blue semiconductor lighting chip and color conversion phosphors are mixed together. Then, conversion phosphors absorb part of the blue light and

emit green, yellow and/or red light to generate abundant visible colors based on the trichromatic theory [22–26]. Inspired by these works in LED color tuning, we propose that multicolor persistent spectral tuning can also be realized by color conversion. Here, CAO is chosen as a persistent donor as it is currently the most efficient blue persistent phosphor [19].  $\text{Ce}^{3+}$ -doped lutetium aluminum garnet ( $\text{Lu}_3\text{Al}_5\text{O}_{12}:\text{Ce}^{3+}$ , LuAG), which is one of the most efficient green color conversion phosphors in LED industry, is used as a color conversion phosphor [27–29]. We try to tune the blue persistent luminescence by changing the mass ratio of LuAG in CAO/LuAG composite. This color conversion strategy was further explored by using four other conversion phosphors to generate abundant persistent color.

## 2. Experimental

### 2.1. Materials

$\text{Ca}(\text{NO}_3)_2 \cdot 4\text{H}_2\text{O}$ ,  $\text{Al}(\text{NO}_3)_3 \cdot 9\text{H}_2\text{O}$ ,  $\text{HBO}_3$ , urea and nitric acid are AR reagents and used as received. Europium oxide, neodymium oxide, and cerium oxide are 4N reagents and their nitrate solutions are prepared by dissolving oxides in nitric acid. Granular activated charcoal are used to generate weak reductive atmosphere to reduce  $\text{Eu}^{3+}$  and  $\text{Ce}^{4+}$  during annealing. Four commercial phosphors (LMY-4453-C, LMY-5049-C, LAM-R-6534, LAM-R-6831), were purchased from Luming Technology Group Co., LTD (China).

\* Corresponding author.

E-mail address: [zjlisci@jnu.edu.cn](mailto:zjlisci@jnu.edu.cn) (Z. Li).

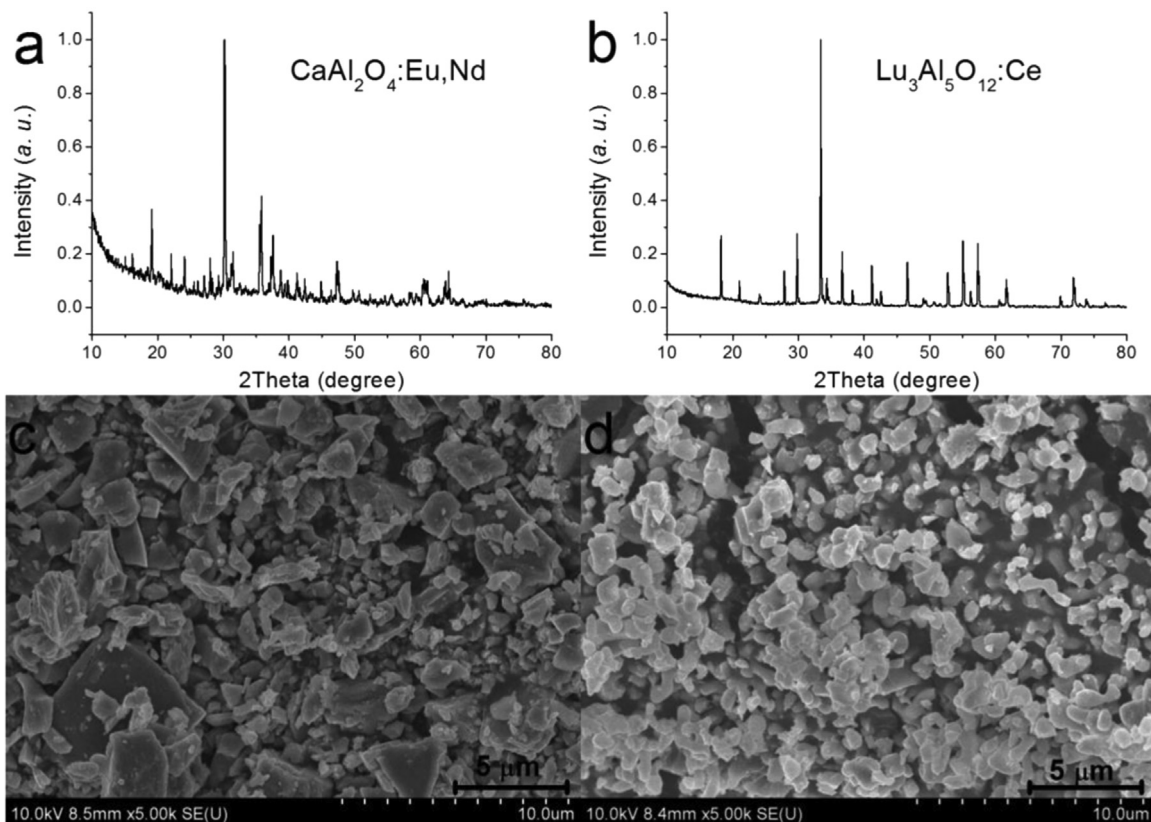


Fig. 1. X-ray diffraction patterns of the as-synthesized CAO persistent phosphor and LuAG phosphor.

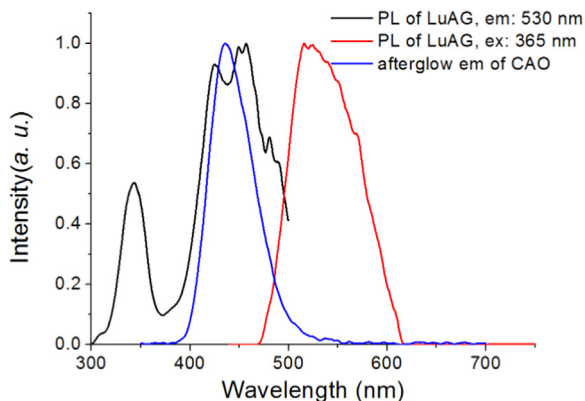


Fig. 2. Photoluminescence and afterglow emission spectra of the as-synthesized LuAG and CAO, respectively.

## 2.2. Synthesis of CAO

The synthesis of CAO was according to a reported sol-gel/combustion method with modifications [30,31]. Briefly,  $\text{Ca}(\text{NO}_3)_2 \cdot 4\text{H}_2\text{O}$ ,  $\text{Al}(\text{NO}_3)_3 \cdot 9\text{H}_2\text{O}$ ,  $\text{HBO}_3$ , urea,  $\text{Eu}(\text{NO}_3)_3$ , and  $\text{Nd}(\text{NO}_3)_3$  were dissolved in deionized water according to a formula of  $(\text{Ca}_{0.97}\text{Eu}_{0.01}\text{Nd}_{0.02})\text{Al}_2\text{O}_4$ . 5% (molar ratio) of  $\text{HBO}_3$  was used as flux. The molar ratio of urea vs. metal ions was 10. The precursor was dried in an oven at  $90^\circ\text{C}$ , forming a xerogel. Then, the xerogel was put into a pre-heated muffle furnace at  $600^\circ\text{C}$  and held in it for 2 h to remove all the organic matter. After cooled to room temperature, the mixture was milled using a mortar and then put into a small corundum crucible with cover. The small crucible was buried into activated carbon in a bigger corundum crucible with cover. The sample was annealed under reductive carbon atmosphere at  $1100^\circ\text{C}$  for 5 h. Finally, CAO powder sample was obtained after the

sample was cooled down to room temperature naturally and milled.

## 2.3. Synthesis of LuAG

LuAG sample was synthesized by using a similar combustion method as that of CAO. The only difference is that the precursor was prepared according to a formula of  $\text{Lu}_{2.97}\text{Ce}_{0.03}\text{Al}_5\text{O}_{12}$ .

## 2.4. Preparation of CAO/LuAG/resin ternary composite chips

CAO/LuAG powder with predetermined mass ratio was mixed with a commercial A/B transparent epoxy resin. The total mass of CAO/LuAG powder was controlled to be 100 mg, while the volume of the used resin controlled to be  $500\ \mu\text{L}$ . The CAO/LuAG/resin mixture was put into a mould with a diameter of 2 cm and kept in the air at room temperature ( $\sim 28^\circ\text{C}$ ) overnight. The resin was solidified and the composite chip was formed after removing the mould. The samples were labeled with the mass content of LuAG (calculated by  $m_{\text{LuAG}}/(m_{\text{LuAG}} + m_{\text{CAO}})$ ).

## 2.5. Characterization

The X-ray diffraction pattern was acquired by using a powder diffractometer with  $\text{Cu K}\alpha$  radiation ( $\lambda = 1.5418\ \text{\AA}$ ) (D2 PHASER, AXS, Germany). The photoluminescence and persistent luminescence spectra were obtained by using a fluorophotometer (Lumina, ThermoFisher, USA). The morphologies were observed by using a field emission scanning electron microscope with an accelerating voltage of 5 kV (S-4800, Hitachi, Japan).

## 3. Results and discussion

As indicated in Fig. 1a, the diffraction pattern of the as-synthesized

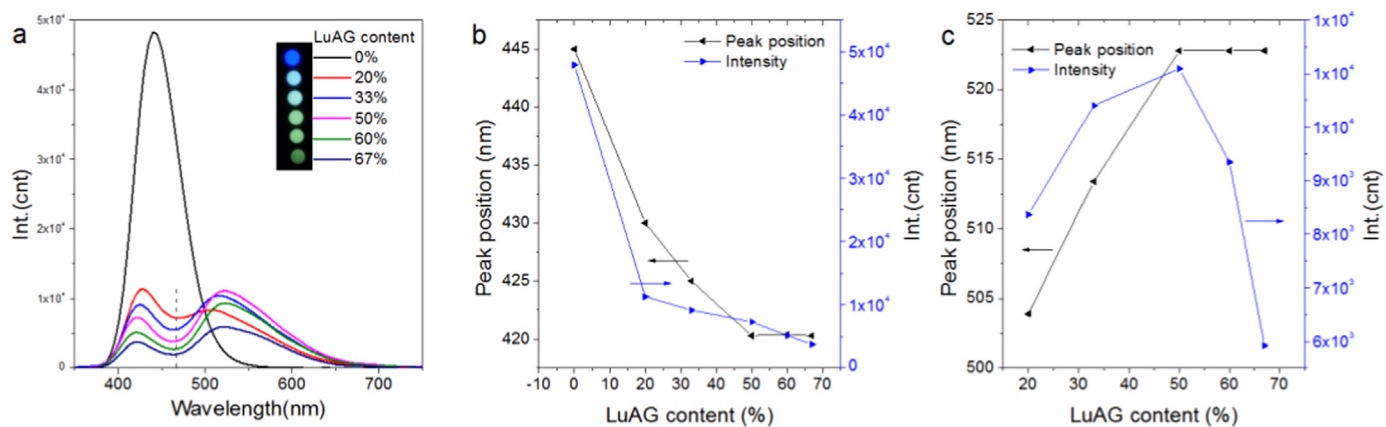


Fig. 3. Persistent luminescence spectra (a) of CAO/LuAG chip samples with diverse LuAG content after irradiation with a violet torch (395 nm, 9 w). The inset picture is a digital picture of the glowing chips in dark. (b) and (c) are the analysis of the blue and green peaks of the spectra, respectively.

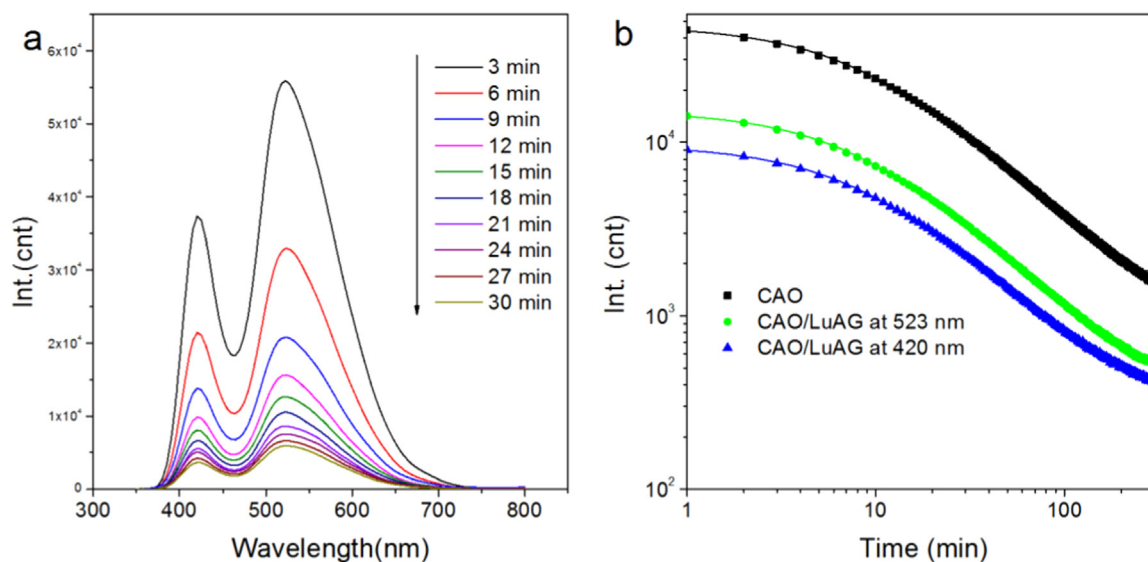


Fig. 4. Persistent luminescence spectra (a) of CAO/LuAG (50%) within 30 min and decay curves (b) of CAO, and CAO/LuAG (50% of LuAG).

Table 1

Fitted parameters of the decay curves of CAO and CAO/LuAG (50% of LuAG) using a dual exponential decay model.

Sample	$\tau_1$ /min	$\tau_2$ /min	R <sup>2</sup>
CAO at 440 nm	8.26	49.47	0.999
CAO/LuAG at 420 nm	8.04	46.56	0.999
CAO/LuAG at 523 nm	8.16	45.83	0.999

Table 2

Photoluminescence information of the commercial phosphors.

Pro. No.	Excitation/nm	Emission/nm
LMY-4453-C	450–470	543
LMY-5049-C	450–470	563
LAM-R-6534	350–550	625
LAM-R-6831	350–550	645

CAO corresponds well with that of monoclinic  $\text{CaAl}_2\text{O}_4$  (JCPDS card no. 23-1036). No apparent impurity diffraction peaks can be observed, indicating the successful doping of Eu and Nd into  $\text{CaAl}_2\text{O}_4$  lattice. The size of CAO particles range from  $\sim 100$  to  $\sim 10$   $\mu\text{m}$ , as shown in Fig. 1c. The as-synthesized LuAG possesses a garnet crystal structure with diffraction pattern corresponding with  $\text{Lu}_3\text{Al}_5\text{O}_{12}$  garnet (JCPDS card no.

731368) (Fig. 1b). The as-synthesized LuAG has a size ranging from  $\sim 200$  to  $\sim 2$   $\mu\text{m}$ . Both CAO and LuAG samples have relatively small sizes which is smaller than most of commercial LED conversion phosphors ( $\sim 10$   $\mu\text{m}$ ). Thus, efficient color conversion may be possible.

In order to establish an efficient color conversion luminescence system, an overlap between donor's emission and acceptor's excitation is a prerequisite. The photoluminescence excitation/emission spectra of LuAG in Fig. 2 indicate that LuAG phosphor can be efficiently excited by a wide spectral range from 400 to 500 nm and emit green light peaking at  $\sim 530$  nm. Notably, its excitation spectrum overlays well with the persistent luminescence spectrum of CAO from 400 to 500 nm with a peak at  $\sim 440$  nm. Therefore, LuAG can serve as a possible efficient conversion phosphor for CAO. In order to study the influence of mass ratio to spectral tuning, CAO/LuAG phosphors with diverse mass ratios were buried into a resin forming thin round chips. The afterglow emission spectra (Fig. 3a) can be divided into two peaks from  $\sim 470$  nm. The “blue” peaks, originating from CAO, decreases along with the increase of LuAG content. The blue emission shifts from  $\sim 440$  to  $\sim 420$  nm, indicating an efficient energy transfer from CAO to LuAG (Fig. 3b). New “green” peaks shift from  $\sim 504$  to  $\sim 523$  nm along with the increase of LuAG content, which can be assigned to the fluorescence emission of LuAG excited by the persistent luminescence of CAO (Fig. 3c). Although greener emission can be obtained by increasing the content of conversion phosphor, LuAG. The persistent luminescence

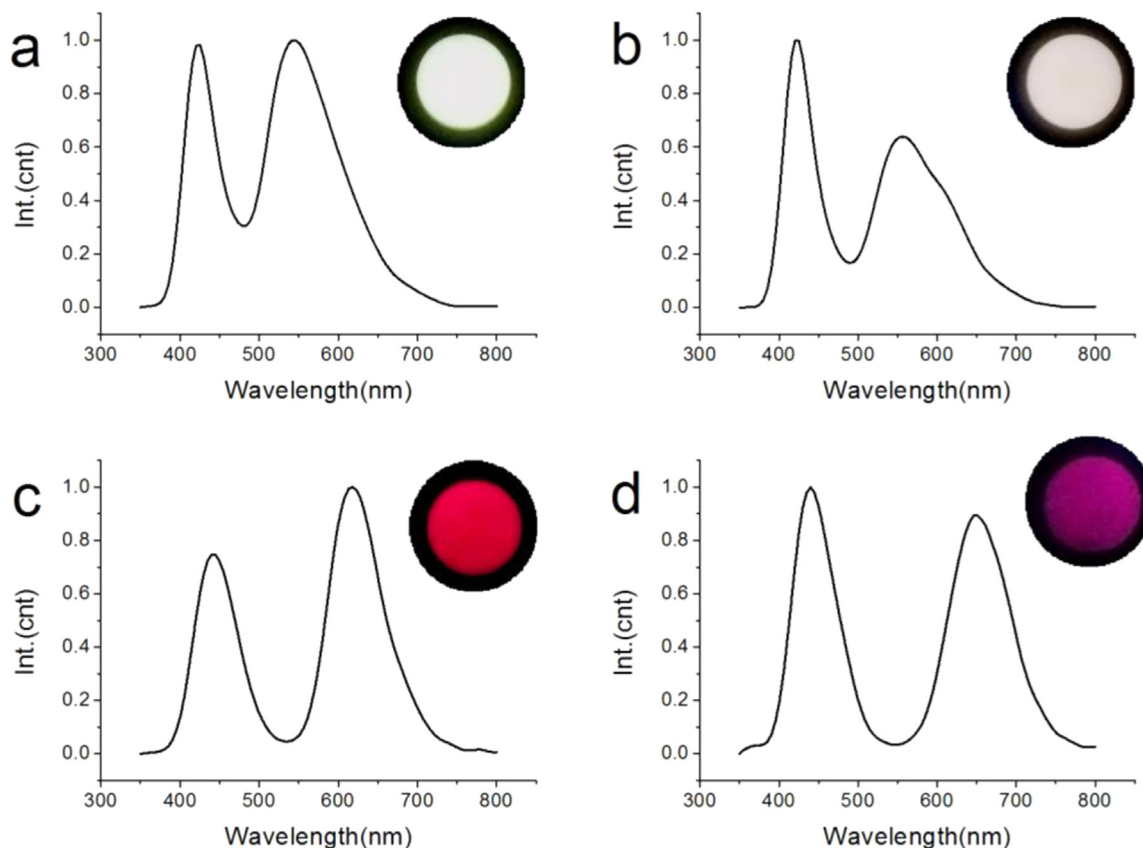


**Fig. 5.** Persistent luminescence spectra of (a) CAO/LMY-4453-C, (b) CAO/LMY-5049-C, (c) CAO/LAM-R-6534, and (d) CAO/LAM-R-6831 sample chips with a conversion phosphor content of 50%. The total CAO/phosphor mass in each chip is 100 mg. The inserted pictures are the afterglow images taken at 10 min after the cessation of LED excitation (395 nm, 9 w, 5 min's irradiation).

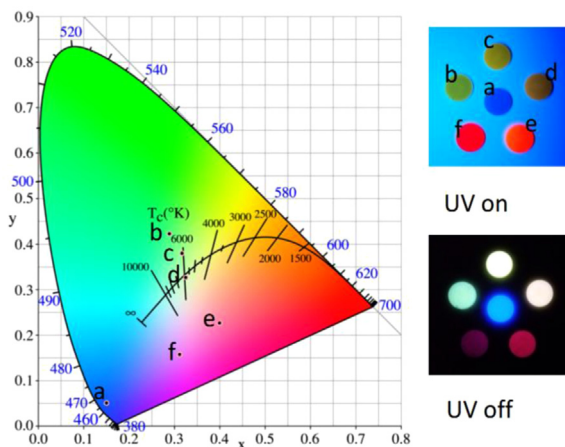


**Fig. 6.** CIE chromaticity diagram and digital pictures of the multicolor CAO/conversion phosphor samples. (a) CAO, (b) CAO/LuAG, (c) CAO/LMY-4453-C, (d) CAO/LMY-5049-C, (e) CAO/LAM-R-6534, and (f) CAO/LAM-R-6831 sample chips. The digital pictures were taken by using a SLR camera after the cessation of LED excitation for 5 min. (For interpretation of the references to color in this figure legend, the reader is referred to the web version of this article).

intensity decreases along with an increasing LuAG content due to less CAO exists. The optimal mass content of LuAG is found to be 50% because of its max emission at 523 nm in all the sample chips.

The afterglow emission color of CAO/LuAG (50% of LuAG) can retain stable during the whole observation period, as shown in Fig. 4a. The persistent luminescence of CAO/LuAG can be detected for more than 5 h (Fig. 4b). Both of the persistent emission at 420 nm and 523 nm

follow dual exponential decay model. In comparison with the decay curve of CAO, CAO/LuAG composite possesses quite similar decay kinetics (Table 1). Therefore, the new persistent emission at 523 nm originates from the persistent excitation of the blue emission of CAO and follows similar decay kinetics of the persistent donor phosphor. The similar values of  $\tau_1$ ,  $\tau_2$  of CAO and CAO/LuAG at 420 nm indicate that there is no significant feedback influence of the converted persistent emission (523 nm) on the blue donor persistent luminescence.

We further explored this color conversion strategy by using several other conversion phosphors, as shown in Table 2. LMY-4453-C and LMY-5049-C are  $\text{Ce}^{3+}$  activated ones with similar crystal structures as that of the as-synthesized LuAG. LAM-R-6534 and LAM-R-6831 are  $\text{Eu}^{2+}$  activated alkaline earth oxynitrides. All these four phosphors are commercial products in LED industry. From their persistent luminescence spectra in Fig. 5, blue shifts of the persistent emission peaks of CAO can be observed in all samples, which is as similar as that of CAO/LuAG sample. New persistent luminescence peaks appears at 543 nm, 556 nm, 617 nm, and 649 nm, corresponding to the fluorescence attributes of the conversion phosphors. These results indicate that this color conversion strategy may be widely applied for tuning persistent luminescence spectra.

Interestingly, the visible color of the samples can be tuned from light green (CAO/LuAG), to light yellow (CAO/LMY-4453-C), and then to white (CAO/LMY-5049-C) (Fig. 6). Regarding to white persistent luminescence,  $\text{Dy}^{3+}$  is usually applied as emitters. However, the 4f-4f transition of  $\text{Dy}^{3+}$  is forbidden and  $\text{Dy}^{3+}$  doped phosphors, such as  $\text{CdSiO}_3:\text{Dy}^{3+}$ , can only be excited by UVC light, which means that it can't be excited efficiently by sunlight or room light and will hinder its practical applications [32]. CAO/LMY-5049-C composite chip possesses bright white persistent luminescence after violet light excitation, which

can be seen for more than 5 h in the dark by naked eyes. Thus, this color conversion strategy may find potential applications in persistent luminescence white LED, anti-fake painting, and safety identification for energy saving lighting applications (Fig. 6). In addition, red persistent luminescence, which is difficult to realize, can be obtained by using red (LAM-R-6534) conversion phosphor. In the case of deep red persistent luminescence, human eyes are relatively not sensitive to deep red emission in the dark. Thus, the persistent luminescence color of CAO/LAM-R-6831 seems violet. All the prepared sample chips can be seen by naked eyes for over 5 h in the dark.

#### 4. Conclusion

CAO, an efficient blue persistent phosphor can serve as an efficient persistent energy donor to excite phosphors without persistent properties. Continuous color tuning persistent luminescence composite material or device can be obtained by simply changing the mass ratio of the donor persistent phosphor and conversion phosphor. Multicolor spectral tuning of persistent luminescence can be realized by choosing matched persistent/conversion phosphor pairs using this color conversion strategy. Although this work only extends the persistent luminescence spectra from blue to deep red, we believe that near infrared persistent luminescence may also be realized by using similar strategy. This work will be significant in indicating other persistent/conversion composite materials or nanostructures with abundant spectral properties.

#### Acknowledgments

This research was supported by the Talent Introduction Special Fund (88016676), Scientific Cultivation and Innovation Fund (11617323) of Jinan University, and the National Natural Science Foundation of China (21701052).

#### References

- [1] T. Lecuyer, E. Teston, G. Ramirez-Garcia, T. Maldiney, B. Viana, J. Seguin, N. Mignet, D. Scherman, C. Richard, Chemically engineered persistent luminescence nanoprobes for bioimaging, *Theranostics* 6 (13) (2016) 2488–2524.
- [2] Y. Li, M. Gecevicius, J.R. Qiu, Long persistent phosphors—from fundamentals to applications, *Chem. Soc. Rev.* 45 (8) (2016) 2090–2136.
- [3] J. Wang, Q. Ma, Y. Wang, H. Shen, Q. Yuan, Recent progress in biomedical applications of persistent luminescence nanoparticles, *Nanoscale* 9 (19) (2017) 6204–6218.
- [4] Q.L. Chermont, C. Chaneac, J. Seguin, F. Pelle, S. Maitrejean, J.P. Jolivet, D. Gourier, M. Bessodes, D. Scherman, Nanoprobes with near-infrared persistent luminescence for *in vivo* imaging, *Proc. Natl. Acad. Sci. USA* 104 (22) (2007) 9266–9271.
- [5] L. Zhang, J. Lei, J. Liu, F. Ma, H. Ju, Persistent luminescence nanoprobe for biosensing and lifetime imaging of cell apoptosis via time-resolved fluorescence resonance energy transfer, *Biomaterials* 67 (2015) 323–334.
- [6] Z.W. Pan, Y.Y. Lu, F. Liu, Sunlight-activated long-persistent luminescence in the near-infrared from Cr<sup>3+</sup>-doped zinc gallogermanates, *Nat. Mater.* 11 (1) (2012) 58–63.
- [7] T. Maldiney, A. Bessiere, J. Seguin, E. Teston, S.K. Sharma, B. Viana, A.J.J. Bos, P. Dorenbos, M. Bessodes, D. Gourier, D. Scherman, C. Richard, The *in vivo* activation of persistent nanophosphors for optical imaging of vascularization, tumours and grafted cells, *Nat. Mater.* 13 (4) (2014) 418–426.
- [8] Z.J. Li, Y.W. Zhang, X. Wu, L. Huang, D.S. Li, W. Fan, G. Han, Direct aqueous-phase synthesis of sub-10 nm "Luminous Pearls" with enhanced *in vivo* renewable near-infrared persistent luminescence, *J. Am. Chem. Soc.* 137 (16) (2015) 5304–5307.
- [9] J.P. Shi, M. Sun, X. Sun, H.W. Zhang, Near-infrared persistent luminescence hollow mesoporous nanospheres for drug delivery and *in vivo* renewable imaging, *J. Mater. Chem. B* 4 (48) (2016) 7845–7851.
- [10] L.J. Chen, C.X. Yang, X.P. Yan, Liposome-coated persistent luminescence nanoparticles as luminescence trackable drug carrier for chemotherapy, *Anal. Chem.* 89 (13) (2017) 6936–6939.
- [11] Z. Xue, X. Li, Y. Li, M. Jiang, H. Liu, S. Zeng, J. Hao, X-ray-activated near-infrared persistent luminescent probe for deep-tissue and renewable *in vivo* bioimaging, *ACS Appl. Mater. Interfaces* 9 (27) (2017) 22132–22142.
- [12] J. Ueda, K. Kuroishi, S. Tanabe, Bright persistent ceramic phosphors of Ce<sup>3+</sup>-Cr<sup>3+</sup>-codoped garnet able to store by blue light, *Appl. Phys. Lett.* 104 (10) (2014) 101904.
- [13] F. Liu, Y.J. Liang, Y.F. Chen, Z.W. Pan, Divalent nickel-activated gallate-based persistent phosphors in the short-wave infrared, *Adv. Opt. Mater.* 4 (4) (2016) 562–566.
- [14] Y. Li, Y.Y. Li, K. Sharafudeen, G.P. Dong, S.F. Zhou, Z.J. Ma, M.Y. Peng, J.R. Qiu, A strategy for developing near infrared long-persistent phosphors: taking MAIO<sub>3</sub>:Mn<sup>4+</sup>, Ge<sup>4+</sup> (M = La, Gd) as an example, *J. Mater. Chem. C* 2 (11) (2014) 2019–2027.
- [15] H.J. Guo, Y.H. Wang, G. Li, J. Liu, P. Feng, D.W. Liu, Cyan emissive super-persistent luminescence and thermoluminescence in BaZrSi<sub>3</sub>O<sub>9</sub>: Eu<sup>2+</sup>, Pr<sup>3+</sup> phosphors, *J. Mater. Chem. C* 5 (11) (2017) 2844–2851.
- [16] W.Z. Sun, R. Pang, H.M. Li, D. Li, L.H. Jiang, S. Zhang, J.P. Fu, C.Y. Li, Investigation of a novel color tunable long afterglow phosphor KGaGeO<sub>4</sub>:Bi<sup>3+</sup>: luminescence properties and mechanism, *J. Mater. Chem. C* 5 (6) (2017) 1346–1355.
- [17] M. Palner, K.Y. Pu, S. Shao, J.H. Rao, Semiconducting polymer nanoparticles with persistent near-infrared luminescence for *in vivo* optical imaging, *Angew. Chem. Int. Ed.* 54 (39) (2015) 11477–11480.
- [18] X.G. Yang, D.P. Yan, Long-afterglow metal-organic frameworks: reversible guest-induced phosphorescence tunability, *Chem. Sci.* 7 (7) (2016) 4519–4526.
- [19] K. Van den Beekhout, P.F. Smet, D. Poelman, Persistent luminescence in Eu<sup>2+</sup>-doped compounds: a review, *Materials* 3 (4) (2010) 2536–2566.
- [20] Y.X. Zhuang, Y. Katayama, J. Ueda, S. Tanabe, A brief review on red to near-infrared persistent luminescence in transition-metal-activated phosphors, *Opt. Mater.* 36 (11) (2014) 1907–1912.
- [21] Z.G. Xia, Q.L. Liu, Progress in discovery and structural design of color conversion phosphors for LEDs, *Prog. Mater. Sci.* 84 (2016) 59–117.
- [22] F. Palazon, F. Di Stasio, Q.A. Akkerman, R. Krahne, M. Prato, L. Manna, Polymer-free films of inorganic halide perovskite nanocrystals as UV-to-white color-conversion layers in LEDs, *Chem. Mater.* 28 (9) (2016) 2902–2906.
- [23] P. Pust, V. Weiler, C. Hecht, A. Tucks, A.S. Wochnik, A.K. Henss, D. Wiechert, C. Scheu, P.J. Schmidt, W. Schnick, Narrow-band red-emitting Sr[LiAl<sub>3</sub>N<sub>4</sub>]:Eu<sup>2+</sup> as a next-generation LED-phosphor material, *Nat. Mater.* 13 (9) (2014) 891–896.
- [24] H. Huang, B.K. Chen, Z.G. Wang, T.F. Hung, A.S. Susha, H.Z. Zhong, A.L. Rogach, Water resistant CsPbX<sub>3</sub> nanocrystals coated with polyhedral oligomeric silsesquioxane and their use as solid state luminophores in all-perovskite white light-emitting devices, *Chem. Sci.* 7 (9) (2016) 5699–5703.
- [25] J.H. Oh, H. Kang, Y.J. Eo, H.K. Park, Y.R. Do, Synthesis of narrow-band red-emitting K<sub>2</sub>SiF<sub>6</sub>:Mn<sup>4+</sup> phosphors for a deep red monochromatic LED and ultrahigh color quality warm-white LEDs, *J. Mater. Chem. C* 3 (3) (2015) 607–615.
- [26] W.B. Chen, Y.H. Wang, W. Zeng, S.C. Han, G. Li, H.J. Guo, Y.Y. Li, Q.P. Qiang, Long persistent composite phosphor CaAl<sub>2</sub>O<sub>4</sub>:Eu<sup>2+</sup>, Nd<sup>3+</sup>/Y<sub>3</sub>Al<sub>5</sub>O<sub>12</sub>:Ce<sup>3+</sup>: a novel strategy to tune the colors of persistent luminescence, *New J. Chem.* 40 (1) (2016) 485–491.
- [27] G.G. Li, Y. Tian, Y. Zhao, J. Lin, Recent progress in luminescence tuning of Ce<sup>3+</sup> and Eu<sup>2+</sup>-activated phosphors for pc-WLEDs, *Chem. Soc. Rev.* 44 (23) (2015) 8688–8713.
- [28] J. Li, S. Sahi, M. Groza, Y.B. Pan, A. Burger, R. Kenarangui, W. Chen, Optical and scintillation properties of Ce<sup>3+</sup>-doped LuAG and YAG transparent ceramics: a comparative study, *J. Am. Ceram. Soc.* 100 (1) (2017) 150–156.
- [29] S.P. Liu, X.Q. Feng, M. Nikl, L.X. Wu, Z.W. Zhou, J. Li, H.M. Kou, Y.P. Zeng, Y. Shi, Y.B. Pan, Fabrication and scintillation performance of nonstoichiometric LuAG:Ce ceramics, *J. Am. Ceram. Soc.* 98 (2) (2015) 510–514.
- [30] C.L. Zhao, D.H. Chen, Synthesis of CaAl<sub>2</sub>O<sub>4</sub>:Eu, Nd long persistent phosphor by combustion processes and its optical properties, *Mater. Lett.* 61 (17) (2007) 3673–3675.
- [31] Q.L. Ma, B.G. Zhai, Y.M. Huang, Effect of sol-gel combustion temperature on the luminescent properties of trivalent Dy doped SrAl<sub>2</sub>O<sub>4</sub>, *Ceram. Int.* 41 (4) (2015) 5830–5835.
- [32] Y.L. Liu, B.F. Lei, C.S. Shi, Luminescent properties of a white afterglow phosphor CdSiO<sub>3</sub>:Dy<sup>3+</sup>, *Chem. Mater.* 17 (8) (2005) 2108–2113.